Available online at www.sciencedirect.com

SciVerse ScienceDirect

Ceramics International 38 (2012) 3141–3147

CERAMICS INTERNATIONAL

www.elsevier.com/locate/ceramint

Calcium carbonate thermal decomposition in white-body wall tile during firing. II. Influence of body thickness and calcite content

A. Escardino *, J. Garcia-Ten, C. Feliu, A. Gozalbo

Instituto de Tecnología Cerámica, Asociación de Investigación de las Industrias Cerámicas, Universitat Jaume I, Castellón, Spain

Received 28 November 2011; received in revised form 7 December 2011; accepted 7 December 2011
Available online 14 December 2011

Abstract

The thermal decomposition process of the calcium carbonate (calcite powder) contained in porous ceramic pieces, with the same composition as that used industrially to manufacture white-firing wall tile bodies, was studied using test disks with different thicknesses and calcite concentrations.

The experiments were conducted in a CO_2-free air atmosphere, and the results confirmed the validity of the kinetic model and the equation proposed in a previous paper to reproduce the experimental results in the studied range of operating conditions.

Keywords: A. Firing; Calcium carbonate; Thermal decomposition; Wall tiles

1. Introduction

1.1. Object of this research

The thermal decomposition of the calcite particles contained in test disks of the same composition and characteristics as those used in this study, was examined in a previous paper [1]. In that study the process was developed in an air atmosphere free of CO_2 at several temperatures, using test disks with the same thickness and calcite content and three different initial porosities. The experimental results were fitted using an equation derived on applying the Shrinking Unreacted Core Kinetic Model [2,3].

In order to complete the study, this paper reports the findings on applying that equation when the process was developed, in a CO_2-free atmosphere, using test disks with different thicknesses and calcite contents and when the process was conducted at two different temperatures from those tested in the previous paper.

1.2. Background

The equation used in the previous paper was of the form:

$$\frac{dX}{dt} = \left(\frac{1}{L \cdot c_B^0}\right) \cdot \left[\frac{K_C - c_Q^G}{(K_C \cdot S_S)/(k \cdot S_i \cdot (1-X)^{1/3}) + (L \cdot X)/(4 \cdot D_e)}\right] \quad (1)$$

This equation relates the conversion degree of the calcium carbonate contained in test disks (X) with residence time (t) and the different operating variables. In this equation c_Q^G represents the CO_2 molar concentration in the gaseous phase during the process. The other symbols are explained in the *Nomenclature*.

Eq. (1) was obtained by assuming that the overall process rate was simultaneously influenced by the rate at which the (reversible) chemical reaction and the diffusion step of the gaseous reaction product (carbon dioxide) from the reaction interface to the surface of the piece unfolded and that mass transfer from the test–disk interface to the gas phase did not influence the overall process rate.

* Corresponding author.
E-mail address: a.escardino@itc.uji.es (A. Escardino).

0272-8842/$36.00
doi:10.1016/j.ceramint.2011.12.016

Nomenclature

Symbols

c_B^0	initial molar concentration of $CaCO_3$ in the test disk (kmol/m^3)
c_Q^G	molar concentration of CO_2 in the gas phase (kmol/m^3)
d_{ap}	test disk dry bulk density (kg/m^3)
D_e	effective overall diffusivity of CO_2 through the solid reacted layer (m^2/min)
k	rate constant of the direct reaction (kmol/(m^2 min)) in Eq. (1)
K_C	chemical equilibrium constant (kmol/m^3) of the reaction in Eq. (1)
L	test disk initial thickness (m)
R	gas constant [0.082 atm m^3/(kmol K)]
S_i	reaction interface area (m^2)
S_s	cross-sectional area of the test disk (m^2)
t	reaction time (min)
T	temperature (K)
X	$CaCO_3$ degree of conversion

Greek letters

ε_0	test disk initial porosity

As the experiments were performed in air atmosphere ($c_Q^G = 0$), the above equation was used in the form:

$$\frac{dX}{dt} = \left(\frac{1}{L \cdot c_B^0}\right) \cdot \left[\frac{K_C}{(K_C \cdot S_s)/(k \cdot S_i \cdot (1-X)^{1/3}) + (L \cdot X)/(4 \cdot D_e)}\right] \quad (2)$$

In that study it was observed that, in the lowest range of calcite conversion degrees under the different tested operating conditions, the experimental results fitted well to the following equation:

$$\frac{dX}{dt} = \left(\frac{1}{L \cdot c_B^0}\right) \cdot \left[\frac{k \cdot S_i (1-X)^{1/3}}{S_s}\right] \quad (3)$$

which derives from Eq. (2) when the overall process rate is only controlled by the rate of the chemical reaction step of calcium carbonate decomposition.

On the other hand, in the highest range of conversion degrees, the experimental results fitted better to Eq. (2) when this was applied starting from a pair of values ($X = X_{02}$; $t = t_{02}$) chosen by trial and error from those resulting from the integration of Eq. (3), as described in that paper [1].

Under constant temperature conditions, it was possible analytically to integrate Eqs. (2) and (3).

Eq. (3) gives

$$t = t_0 + \frac{3 \cdot S_s \cdot L \cdot c_B^0}{2 \cdot k \cdot S_i} \cdot \left[1 - (1-X)^{2/3}\right] \quad (4)$$

where t_0 (induction time) is the time that the test disk took to reach the operating temperature in each experiment, which was determined from the experimental data in the form described elsewhere [1].

Integrating Eq. (2), starting from the boundary conditions ($X = X_{02}$; $t = t_{02}$) indicated above, gives:

$$t = t_{02} + \frac{3 \cdot S_s \cdot L \cdot c_B^0}{2 \cdot k \cdot S_i} \cdot \left[(1-X_{02})^{2/3} - (1-X)^{2/3}\right] + \frac{L^2 \cdot c_B^0}{4 \cdot D_e \cdot K_C} \cdot \left[\frac{X^2}{2} - \frac{X_{02}^2}{2}\right] \quad (5)$$

2. Materials and experimental procedure

2.1. Materials

The test disks (cylindrical pieces, 40 mm in diameter and 7 mm thick) used to conduct this study were formed by uniaxial pressing from the same mixture of natural raw materials as that used in the previous paper, consisting of clay (60%), feldspathic sand (25%) and calcite (15%). The oxide composition of each raw material used is detailed in Table 1. The average radius of the calcite particles used to prepare these mixtures was 3.5 μm. Pressing powder moisture content was kept constant at 0.055 kg water/kg dry solid.

2.2. Experimental assembly and procedure

The calcium carbonate decomposition reaction was monitored by measuring sample weight loss during isothermal treatment in a laboratory tubular kiln. Air was fed into the kiln at a controlled temperature and flow rate. The assembly (Fig. 1) consisted of a refractory steel sample-holder, set in the middle of the kiln firing chamber. The holder was suspended from a single-pan balance by an alumina rod, so that sample mass could be continuously measured. The balance was connected to a computer with the appropriate software to record the pairs of mass–time values.

The test pieces were preheated for 30 min, in carbon dioxide atmosphere, in an oven that ran at 400 °C. The side of each test piece was sealed with a glaze to prevent any lateral CO_2 losses

Table 1
Chemical composition, expressed in % by weight of oxides, of the raw materials used.

Oxide	Clay	Feldspathic sand	Calcite
SiO_2	64.6	88.5	0.2
Al_2O_3	22.1	6.5	0.1
Fe_2O_3	2.11	0.15	0.05
TiO_2	1.10	0.08	–
Na_2O	0.15	0.13	–
K_2O	2.00	2.84	0.01
CaO	0.23	0.17	55.7
MgO	0.28	<0.01	0.20
P_2O_5	0.10	0.02	0.11
MnO	0.01	–	0.01
L.O.I.	7.20	1.54	43.5

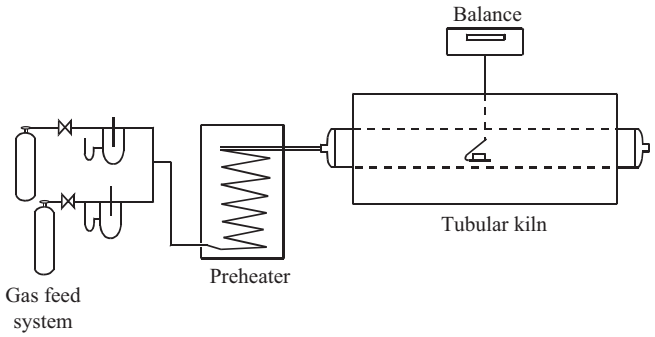

Fig. 1. Experimental assembly.

during thermal treatment, so that the gaseous product would only be released through the two faces of the disk.

The rest of the procedure used has been described in the previous paper (Sections 2.3, 3.1, and 3.2) [1].

3. Experimental results and discussion

All the decomposition experiments were conducted under isothermal conditions, and the gaseous mixture was circulated through the reactor at a sufficiently high flow rate to ensure that mass transfer from the test–disk interface to the gas phase would not influence the overall process rate [1].

In the previous paper, under the tested operating conditions, using test disks analogous to those studied in this paper, it was found that the product $(k{\cdot}S_i)$ and the diffusivity D_e, in the above equations, varied exponentially with operating temperature and with initial porosity of the test disks (ε_0), according to the equations:

$$k \cdot S_i = 0.866 \cdot \exp\left(-\frac{119689}{8.314 \cdot T}\right) \tag{6}$$

$$D_e = 5.277 \cdot 10^{-4} \cdot \exp(15.34 \cdot \varepsilon_0) \cdot \exp\left[-\frac{5189 \cdot \exp(0.563 \cdot \varepsilon_0)}{T}\right] \tag{7}$$

where the temperature (T) is expressed in K.

The values of the product $(k{\cdot}S_i)$ were determined instead of those of k, because the interface surface area (S_i) corresponding to the chemical reaction step was not precisely known.

It was also observed that the conversion degree of the calcium carbonate contained in the disk ($X = X_{02}$) at which it was necessary to switch from Eq (4) to Eq. (5) to fit the experimental data depended on the operating temperature and on disk initial porosity (ε_0).

The value of the equilibrium constant (K_C) at each temperature was determined, applying the law of gases, starting from the value of the thermal dissociation pressure of calcium carbonate (P_Q^0) at the same temperature T (K), from the following equation [4]:

$$K_C = \frac{P_Q^0}{R \cdot T} = \frac{(1.3158 \cdot 10^{-3}) \cdot (10^{10.4022 - 8792.3/T})}{R \cdot T} \tag{8}$$

3.1. Influence of test disk thickness

Four experiments were conducted to study the influence of test disk thickness, varying disk thickness in each, while keeping the following operating conditions constant: reaction temperature: 875 °C (1148 K); disk calcite content: 15.0% (by weight); and disk dry bulk density: 1950 kg/m^3 ($\varepsilon_0 = 0.267$). The tested disk thicknesses (L) were 5.0, 7.0, 9.0, and 12.0 mm. In all experiments, CO_2-free air was passed through the reactor.

The results are plotted in the form $X = f(t)$ in Fig. 2.

Fig. 2 shows that when disk thickness was increased, keeping the other operating conditions constant, the slope of the $X = f(t)$ plots decreased, which agrees qualitatively with Eqs. (2) and (3).

Since the experiments were conducted under isothermal conditions in an air stream without carbon dioxide, Eqs. (4) and (5) were used in order to attempt to correlate the experimental data plotted in these figures.

When the value of the product $(k{\cdot}S_i) = 3.1 \cdot 10^{-6}$ corresponding to the operating temperature used (1148 K), calculated from Eq. (6), and the values of $c_B^0 = 2.925\,\text{kmol/m}^3$ and $S_s = 0.00125\,\text{m}^2$, corresponding to the characteristics of the test disks, together with the respective disk thickness (L), were substituted in Eq. (4), the experimental X–t values corresponding to the lowest range of conversion degrees were reproduced well, as may be observed in Fig. 2 (dashed lines).

Eq. (5) was then applied to the experimental data corresponding to the highest range of conversion degrees, substituting the value of $K_C = 0.0081$, calculated from Eq. (8) at the operating temperature (1148 K), together with the values of c_B^0, S_s, and $(k{\cdot}S_i)$ mentioned above, trying out different effective diffusivity (D_e) values, taking as the starting point 0.000235 m^2/min calculated from Eq. (7) for the initial

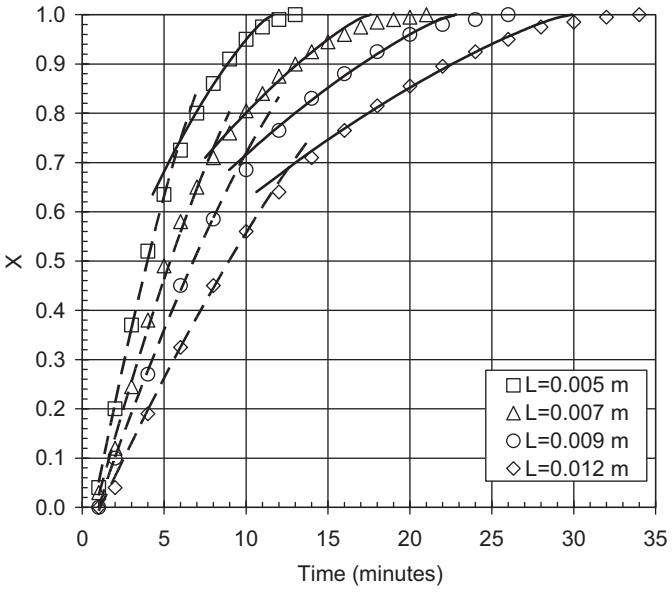

Fig. 2. Influence of test disk thickness (L). Fit of the experimental data to Eqs. (4) (dashed lines) and (5) (solid lines). $d_{ap} = 1950\,\text{kg/m}^3$ ($\varepsilon_0 = 0.267$); $c_B^0 = 2.925\,\text{kmol/m}^3$; $T = 875$ °C.

Table 2
Values of X_{02} and t_{02} obtained in the best fits of Eqs. (4) and (5), together with the corresponding values of L {$T = 875$ °C; $S_s = 0.00125$ m^2; $d_{ap} = 1950$ kg/m^3 ($\varepsilon_0 = 0.267$); 15.0% calcite by weight ($c_B^0 = 2.925$ kmol/m^3)}.

L (m)	t_0 (min)	t_{02} (min)	X_{02}	D_e (m^2/min)
0.0050	0.7	6.0	0.746	0.000235
0.0070	0.8	8.0	0.729	0.000235
0.0090	0.9	9.8	0.710	0.000300
0.0120	1.1	12.6	0.690	0.000450

porosity of the disks ($\varepsilon_0 = 0.267$) and for the operating temperature used ($T = 1148$ K) until the best fit to the experimental data was achieved.

In this case as well, the pairs of X–t values calculated from Eq. (5) fitted well to the experimental data (solid lines in Fig. 2), with the reservations noted below.

Table 2 presents the respective values of X_{02} and t_{02} obtained by trial and error, corresponding to the X–t pairs of values which required switching from Eq. (4) to Eq. (5), as well as the values of D_e resulting from the best fits to the experimental data, together with the test disk thicknesses (L).

As the table shows, when the fit of Eq. (5) to the experimental results corresponding to disk thicknesses of 0.005 and 0.007 m was optimised, the same value (0.000235 m^2/min) was obtained for effective diffusivity D_e, which coincided with the value previously calculated with Eq. (7) under the corresponding disk initial porosity and operating temperature conditions. In contrast, when the fit to the experimental results corresponding to disk thicknesses of 0.009 and 0.012 m was optimised, the values 0.00030 and 0.00045 m^2/min were obtained, respectively, for effective diffusivity (D_e), which were slightly higher than the value calculated from Eq. (7).

The observed increase in the value of D_e, with respect to the expected value from Eq. (7) for disk thicknesses (L) ≥ 0.009 m, might be due to the influence of the pressure gradients that developed throughout the test disk during disk forming by uniaxial dry pressing making the disk more permeable as disk thickness increased [5].

The observed increase in D_e for the two highest studied disk thicknesses might also be caused by the need for the disks to remain longer in the reactor as disk thickness increased, in order to complete the thermal decomposition of the calcite content. Longer disk residence time at high temperature favours disk sintering progress, increasing the pore radius and, hence, the disk coefficient of permeability [6], which is directly related to effective diffusivity.

On the other hand, as Table 2 shows, when disk thickness increased, the conversion degree at which the diffusion stage began to have an influence (X_{02}) decreased. This decrease in X_{02}, which was more pronounced in the case of the two highest studied thicknesses, is in agreement with the model. Thus, when disk thickness (L) increases, the value of the second term of the denominator of the second member of Eq. (2), which represents the resistance opposed by the diffusion stage to the development of the process, rises. As a result, when disk thickness increases, the diffusion stage must begin to influence the overall process rate at lower conversion degrees (X).

3.2. Influence of the $CaCO_3$ content in the test disks

In order to study the influence of this variable, 7.0-mm-thick test disks were prepared with a dry bulk density of 1950 kg/m^3 ($\varepsilon_0 = 0.267$) and different calcite particle contents (varying consequently the clay and feldspathic sand content), by weight, keeping the other disk characteristics and properties constant. These experiments, just as the foregoing thickness experiments, were conducted at 875 °C (1148 K) in air atmosphere. Four calcite contents were tested: 11.0, 13.0, 15.0, and 17.0% by weight, corresponding to calcium carbonate molar concentrations in the disks (c_B^0) of 2.145, 2.535, 2.925, and 3.315 kmol/m^3 disk, respectively.

The results obtained are plotted in the form $X = f(t)$ in Fig. 3.

The plots show that, when the initial calcite concentration in the disks increased, the slope of the $X = f(t)$ curves decreased in accordance with Eqs. (2) and (3).

The methodology described in the previous section was carried out in order to verify whether, on sequentially applying Eqs. (4) and (5), substituting in these equations the values of the operating variables calculated from Eqs. (6)–(8), the experimental results obtained in the four experiments could be predicted.

When Eq. (4) was applied, the values of the product $(k \cdot S_i) = 3.1 \cdot 10^{-6}$, of $K_C = 0.0081$, obtained from Eqs. (6) and (8) at the operating temperature used (1148 K), and of $L = 0.007$ m and $S_s = 0.00125$ m^2, corresponding to the dimensions of the disks involved, were used. When Eq. (5) was applied, the value of $D_e = 0.000235$ m^2/min was also used, calculated from Eq. (7) for the initial porosity ($\varepsilon_0 = 0.267$) and operating temperature ($T = 1148$ K) used, trying out different pairs of values (X_{02}, t_{02}) located on the curve resulting from the

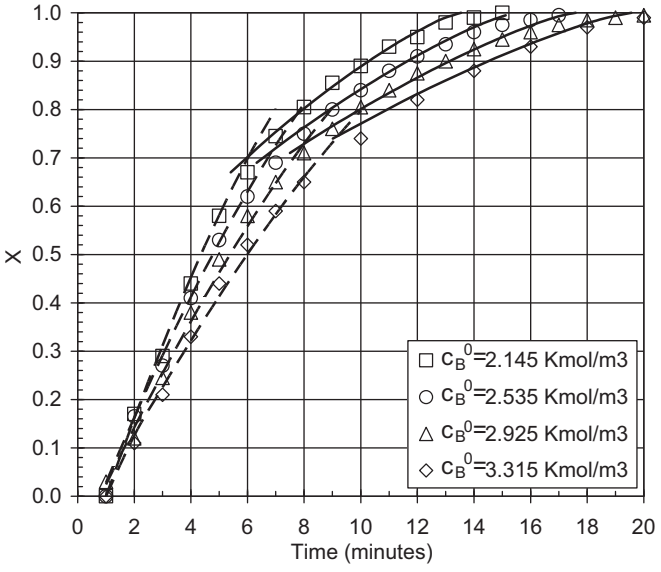

Fig. 3. Influence of calcium carbonate concentration (c_B^0). Fit of the experimental data to Eqs. (4) (dashed lines) and (5) (solid lines). $d_{ap} = 1950$ kg/m^3 ($\varepsilon_0 = 0.267$); $L = 0.007$ m; $T = 875$ °C.

Table 3
Values of X_{02} and t_{02} obtained in the best fits of Eqs. (4) and (5), together with the corresponding values of c_B^0 (T = 875 °C; S_s = 0.00125 m^2; d_{ap} = 1950 kg/m^3 (ε_0 = 0.267); L = 0.007 m).

Calcium carbonate content (% by weight)	c_B^0 (kmol $CaCO_3$/m^3 test disk)	t_0 (min)	t_{02} (min)	X_{02}	D_e (m^2/min)
11.0	2.145	1.0	6.05	0.705	0.000235
13.0	2.535	0.7	6.90	0.716	0.000235
15.0	2.925	0.8	8.00	0.729	0.000235
17.0	3.315	0.8	9.20	0.746	0.000235

application of Eq. (4) and selecting, in each case, the pair of values that provided the best fit of Eq. (5) to the experimental data corresponding to the highest section of conversion degrees.

The X–t curves obtained by sequentially applying Eqs. (4) and (5) for the four experiments performed with different calcite concentrations (c_B^0), substituting the corresponding values of these concentrations in the equations, as well as those of the other operating variables mentioned in the previous paragraph, have been plotted as dashed lines and solid lines respectively, together with the experimental data, in Fig. 3.

It may be observed that the lines representing the pairs of X–t values, calculated by applying the above equations to the two sections being considered in the form mentioned, fit very well to the experimental data, confirming the validity of the model for any initial calcite concentration in the test pieces in the studied range of calcite contents.

The respective pairs of values of X_{02} and t_{02} resulting from the best fits obtained with Eq. (5), together with the corresponding values of t_0, as well as the values of c_B^0 and D_e used, are shown in Table 3.

4. Application of the proposed equations to different operating conditions from those tested previously

In principle, it should be possible to use Eqs. (4) and (5) for predicting the variation of X with t when the studied thermal decomposition process unfolds at constant temperature under different operating conditions from the tested conditions, if the decomposition process takes place within the ranges of values of the operating conditions encompassed in the foregoing sections and in the first part of this study,[1] provided that the calcite particles contained in the green test disks are of the same size, nature, and characteristics as those used in this research, and the process occurs in air atmosphere.

This requires knowing, in each case, the value of the boundary conditions (X_{02}; t_{02}) from which Eq. (5) is to be applied starting from the second reaction period.

4.1. Determination of the boundary conditions (X_{02}; t_{02}) from which Eq. (5) may be applied to the second reaction period

In order to be able to predict the value of one of these two boundary conditions when the process unfolded under different operating conditions from those tested, within the studied range of values for these variables, it was attempted to obtain a correlation between X_{02} or t_{02} and the operating temperature, disk initial porosity, and the calcium carbonate molar concentrations in the compacts, starting with the experimentally obtained pairs of values of these variables.

The values of X_{02}, obtained in the previous paper (Table 4) [1] at the six tested operating temperatures for the three studied initial porosities, have been plotted against the respective operating temperatures, on rectangular coordinates in Fig. 4. As may be observed, practically all the experimental points fell in a straight line for each studied disk initial porosity (ε_0).

These plots were satisfactorily fitted to the following equations:

$$X_{02} = -1.920 + 0.00230 \cdot T \quad (\varepsilon_0 = 0.304) \tag{9}$$

$$X_{02} = -2.481 + 0.00281 \cdot T \quad (\varepsilon_0 = 0.267) \tag{10}$$

$$X_{02} = -2.742 + 0.00303 \cdot T \quad (\varepsilon_0 = 0.229) \tag{11}$$

in which the temperature was expressed in K.

On the other hand, when the values of X_{02} obtained in this study were plotted against the respective disk thicknesses (L) or calcium carbonate molar concentrations (c_B^0) (Tables 2 and 3) on rectangular coordinates, they also satisfactorily fitted to straight lines of equations:

$$X_{02} = 0.785 - 8.07 \cdot L \tag{12}$$

$$X_{02} = 0.628 + 0.0355 \cdot c_B^0 \tag{13}$$

valid for the studied ranges of L, ε_0 and c_B^0 values.

From these equations, knowing the operating temperature and the test disk characteristics (L, ε_0, and c_B^0 values), it should be possible to calculate the corresponding value of X_{02} at which it is necessary to switch from Eqs. (4) and (5) when those are applied.

Table 4
Values of X_{02}, ($k \cdot S_i$), D_e, and K_C, corresponding to each test T, and of c_B^0 and ε_0 of the test disks used (S_s = 0.00125 m^2; L = 0.007 m; 15% calcite by weight).

T (°C)	T (K)	ε_0	c_B^0 (kmol/m^3)	$k \cdot S_i \cdot 10^6$ (kmol/min)	t_0 (min)	K_C (kmol/m^3)	D_e (m^2/min)	X_{02}
837	1110	0.304	2.775	2.018	0.8	0.00438	0.000315	0.658
837	1110	0.267	2.925	2.018	0.8	0.00438	0.000198	0.637
837	1110	0.229	3.075	2.018	0.9	0.00438	0.000123	0.621
887	1160	0.304	2.775	3.530	0.8	0.00920	0.000393	0.748
887	1160	0.267	2.925	3.530	0.7	0.00920	0.000247	0.778
887	1160	0.229	3.075	3.530	0.7	0.00920	0.000153	0.773

4.2. Application of Eqs. (4) and (5) to processes unfolding under isothermal conditions at different temperatures from those studied

In order to verify the validity of Eqs. (4) and (5) and of the proposed methodology for predicting the variation of the conversion degree (X) of the calcium carbonate contained in the test disks with reaction time (t) when different temperature conditions from those studied[1] were used, within the studied range of temperatures (825–950 °C), three series of experiments with different values of ε_0 were conducted at 837 °C, while three other series were carried out at 887 °C. The experimental data are plotted in Figs. 5 and 6, respectively.

In accordance with the foregoing, if in Eqs. (4) and (5) one substitutes the values of L, c_B^0, and ε_0 corresponding to the characteristics of the pieces used, as well as the values of the product $(k{\cdot}S_i)$, of diffusivity D_e, and of the equilibrium constant K_C, calculated at the temperature and initial porosity established in each case from Eqs. (6), (7) and (8), respectively, determining from Eqs. (9)–(11) the value of X_{02} at which it is necessary to switch equations during the integration, pairs of X–t values must be obtained that, when plotted in Figs. 5 and 6, should be superposed on the experimental data points.

Test disk characteristics and the values of kinetic parameters $(k{\cdot}S_i)$, D_e, K_C, and X_{02}, calculated at the two test temperatures from Eqs. (6) to (11), are presented in Table 4.

Operating in the form described above, the X–t pairs of values corresponding to the six series of experiments conducted were calculated. Induction time t_0 was determined in each case by trial and error, as in the previous paper,[1] from the best fit of Eq. (4) to the experimental data.

The calculated values have been plotted in Figs. 5 and 6 by means of dashed and solid lines. The first section of these lines (i.e. the dashed lines) corresponds to the values calculated from Eq. (4), while the second section (i.e. the solid lines) corresponds to the values calculated from Eq. (5). The agreement between the experimental data and the calculated values is excellent, which confirms the effectiveness of the equations and of the proposed methodology for predicting the variation of the degree of conversion of the calcium carbonate contained in the studied test disks with residence time, at any temperature, when the process is carried out under isothermal conditions in the studied range of operating conditions in air atmosphere.

Only in the experiment at a temperature of 837 °C and an initial porosity of 0.304 was it necessary slightly to modify the value of X_{02} calculated from Eq. (9), the calculated value being

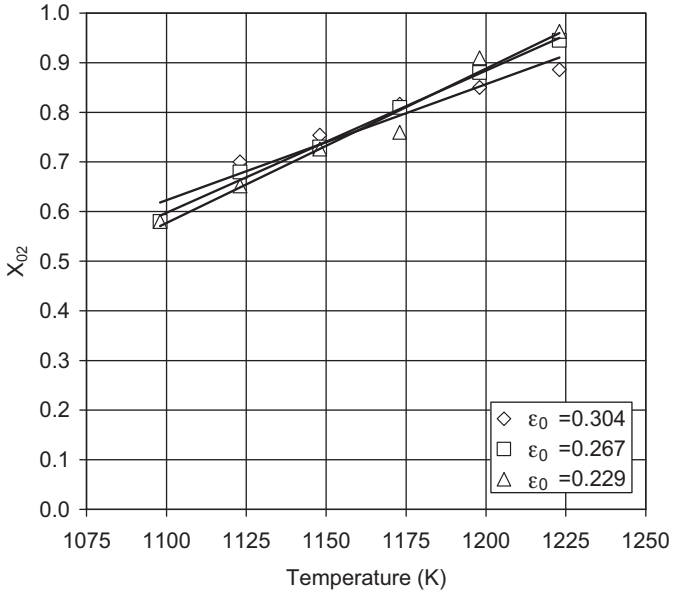

Fig. 4. Variation of X_{02} with operating temperature (K).

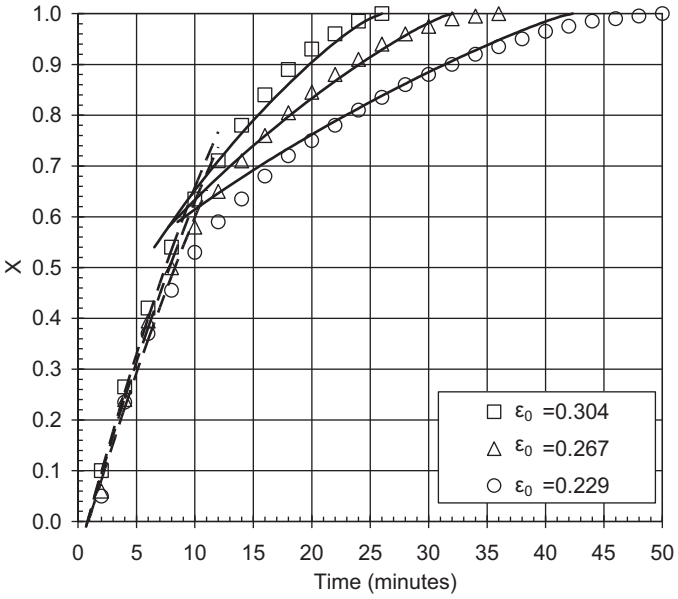

Fig. 5. Fit of the experimental data to Eqs. (4) (dashed lines) and (5) (solid lines). T = 837 °C; L = 0.007 m.

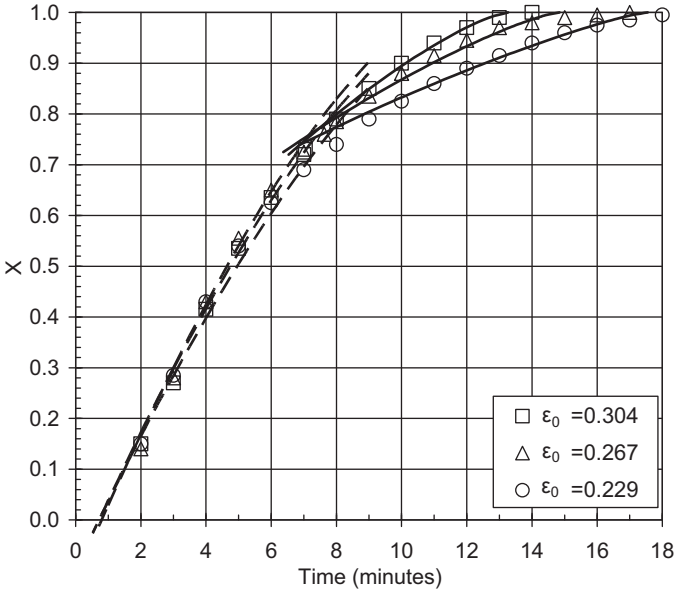

Fig. 6. Fit of the experimental data to Eqs. (4) (dashed lines) and (5) (solid lines). T = 887 °C; L = 0.007 m.

0.633, while the modified value was 0.658, in order to improve the fit of Eq. (5) to the experimental results.

5. Conclusions

The validity of the proposed equations to fit the experimental data of calcium carbonate thermal decomposition in white-body wall tile during firing was confirmed for ceramic test disks of varying thicknesses and the same composition; of varying calcite contents and the same thickness; in addition to two different operating temperatures from those tested in the previous paper, within the range of 825–950 °C, when the process was carried out in air atmosphere.

Acknowledgements

The authors thank the Instituto de la Mediana y Pequeña Empresa de Valencia (IMPIVA) of the Generalitat Valenciana for its financial help. They are also grateful for the support of ERDF funds from the European Union. Project reference IMIDIC/2007/102.

References

[1] A. Escardino, J. García-Ten, C. Feliu, A. Moreno, Calcium carbonate thermal decomposition in white-body wall tile during firing. I. Kinetic study, J. Eur. Ceram. Soc. 30 (2010) 1989–2001.
[2] L.K. Doraiswamy, M.M. Sharma, Heterogeneous Reactions: Analysis, Examples, and Reactor Design: Gas–Solid and Solid–Solid Reactions, vol. 1, John Wiley and Sons, New York, 1984, pp. 450–456.
[3] O. Levenspiel, The Chemicals Reactor omnibook, St. Univ Bookstores, Oregon, 1996, pp. 55.3–55.4.
[4] K.J. Hill, E.R.S. Winter, Thermal dissociation pressure of calcium carbonate, J. Phys. Chem. 60 (1956) 1361–1362.
[5] J.S. Reed, Principles of Ceramics Processing, 2nd ed., John Wiley and Sons, New York, 1995, pp. 436–440.
[6] T. García-Ten, Descomposición, durante la cocción, del carbonato cálcico contenido en el soporte crudo de los azulejos, PhD dissertation, Castellón (Spain), Universitat Jaume I, 2005.